

## ac relaxation mechanism in some cuprate glasses

S. Hazra and A. Ghosh\*

*Department of Solid State Physics, Indian Association for the Cultivation of Science, Calcutta 700 032, India*

(Received 7 February 1995; revised manuscript received 15 November 1996)

Electrical conductivity and dielectric properties of some unconventional lead cuprate glasses have been reported in the temperature range of 80–550 K and in the frequency range  $10^2$ – $10^6$  Hz. The experimental data have been analyzed in the light of different theoretical models. It has been observed that at low temperatures, the ac conductivity is much higher than the dc conductivity and the hopping of electrons between localized states near the Fermi level is the dominant loss mechanism. At higher temperatures, the ac conductivity approaches the dc conductivity and the dipolar relaxation model with a distribution of relaxation times can give the best description of the experimental data. Dipolar relaxation occurs due to the hopping of charge carriers within a range of energies near the mobility edge. The conductivity relaxation model provides satisfactory values of low- and high-frequency dielectric constants and dc conductivity. On the other hand, the random-free-energy-barrier model is not consistent with the dielectric data. The unconventional glass network former PbO gives rise to large values of the low- and high-frequency dielectric constants and a narrower distribution of relaxation times than the conventional network formers. [S0163-1829(97)03410-3]

### I. INTRODUCTION

Like many other amorphous materials,<sup>1–3</sup> a frequency dependent ac conductivity and loss have been observed in semiconducting glasses containing transition metal ions<sup>4–6</sup> and have been the subject of much controversy. At low temperature, the ac conductivity  $\sigma(\omega)$  at frequency  $\omega$  behaves as  $\omega^s$  where  $s$  is generally less than or equal to unity and depends on temperature. A value of  $s$  higher than unity has also been reported in some cases<sup>7</sup> at low frequencies and temperatures. Several models<sup>1–3</sup> based on the relaxation caused by the hopping or tunneling of electrons or atoms between equilibrium sites have been developed to explain the frequency and temperature dependence of the ac conductivity and  $s$ . However, these models are applicable only within a limited temperature range. Apart from the controversy of the low-temperature behavior of  $\sigma(\omega)$  and  $s$ , there is some uncertainty whether a Debye-type dielectric loss peak exists at high temperatures, where the ac conductivity approaches the dc conductivity.<sup>8</sup> The transition metal ion glasses based on the conventional glass network formers such as  $P_2O_5$ ,  $TeO_2$ , etc., have been studied earlier.<sup>4–7</sup> However, fewer investigations have been made on the influence of the glass network on the ac response.<sup>9</sup> Recently, transition metal ion glasses based on unconventional glass network formers such as  $Bi_2O_3$  and PbO have been reported.<sup>10,11</sup> The purpose of the present work is to study the frequency-dependent conductivity and loss of the well characterized unconventional CuO-PbO glasses of different compositions. It has been observed that the unconventional network former PbO has a strong influence on the dielectric properties in comparison with the conventional network formers.

### II. EXPERIMENTAL PROCEDURE

Glass samples of compositions  $x\text{CuO}-(100-x)\text{PbO}$  (mol %) were prepared, within the glass formation limit  $20 \leq x \leq 50$  (Ref. 11), by melting the reagent grade CuO and PbO in alumina crucibles for 1 h in an electric furnace at a

temperature in the range 1100–1250 °C depending on compositions and subsequently quenching the melts in a twin roller. The amorphous nature of the samples was checked by x-ray diffraction and electron microscopy. The prepared glass compositions were well characterized by a variety of techniques such as differential thermal analysis, density, and molar volume, atomic absorption, infrared absorption, electron spin resonance, etc.<sup>11</sup>

Depending on conductivity levels, the ac measurements were carried out in a GenRad (model-1615A) Capacitance Bridge in the frequency range  $10^2$ – $10^5$  Hz or in a Hewlett Packard (model-4192A LF) Impedance Analyzer in the frequency range  $10^2$ – $10^6$  Hz, using gold as an electrode material. The dc measurements were made in a Keithley (model-617) electrometer. All measurements were taken in the temperature range 80–550 K. The sample cell was placed in an electric furnace and in a cryostat for measurements above and below the room temperature, respectively.

### III. RESULTS

The measured ac conductivity as a function of reciprocal temperature and the dielectric constant as a function of temperature for the 30 CuO-70 PbO glass composition are shown in Figs. 1 and 2, respectively, at three frequencies. The dc conductivity is also included in Fig. 1 for comparison. It is clear in Fig. 1 that at lower temperatures, the ac conductivity is substantially higher than the dc conductivity and shows a weak temperature dependence but a strong frequency dependence, while at higher temperatures, the ac conductivity shows a strong temperature dependence but almost frequency independence approaching the dc conductivity. Figure 2 shows that the dielectric constant  $\epsilon'(\omega)$  is almost independent of temperature below 340 K and shows a weak frequency dispersion. However, it shows a strong temperature dependence and frequency dispersion above this temperature. The temperature, at which the dielectric constant increases rapidly, increases for higher frequencies. The frequency dependence of measured ac conductivity and di-

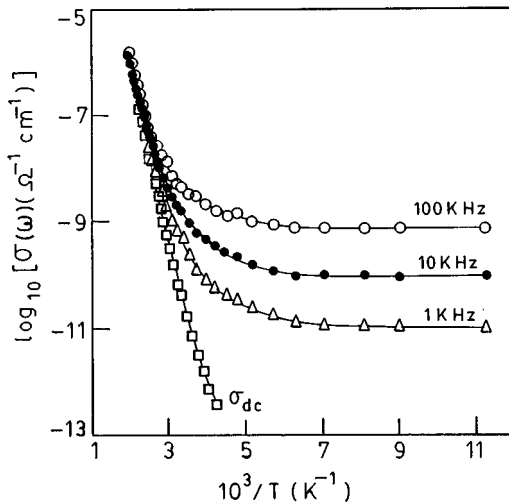


FIG. 1. The temperature dependence of the measured ac conductivity at three different frequencies and dc conductivity for the 30 CuO-70 PbO glass composition. Solid curves are drawn through the data to guide the eye.

electric constant at different temperatures are shown in Figs. 3(a) and 3(b), respectively, for the same glass composition as in Fig. 1. The temperature and frequency dependence of the ac conductivity and dielectric constant for the other glass compositions are qualitatively similar. It may be noted that the dielectric constants of all the glass compositions are much higher than those for the transition metal ion glasses based on conventional network formers such as  $P_2O_5$ .<sup>4,5</sup> This clearly suggests the influence of the unconventional network former PbO on the dielectric properties due to the higher polarizability of  $Pb^{2+}$  ions than that of  $P^{5+}$  ions.

#### IV. DISCUSSION

As seen in Fig. 3(a) the ac conductivity at lower temperatures, where the ac conductivity is substantially higher than the dc conductivity, can be expressed as  $\sigma(\omega) = A\omega^s$ , where

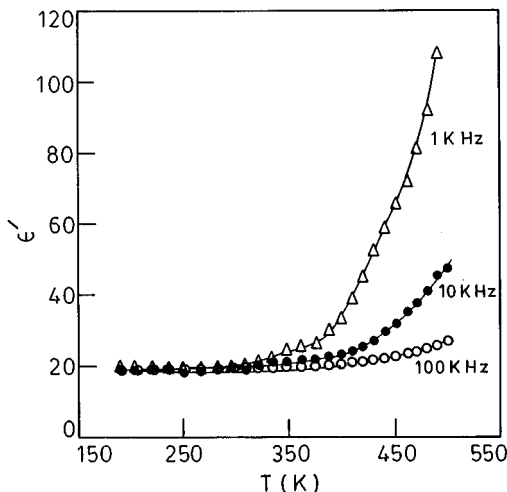


FIG. 2. Variation of dielectric constant,  $\epsilon'$  with temperature for three different frequencies for the 30 CuO-70 PbO glass composition.

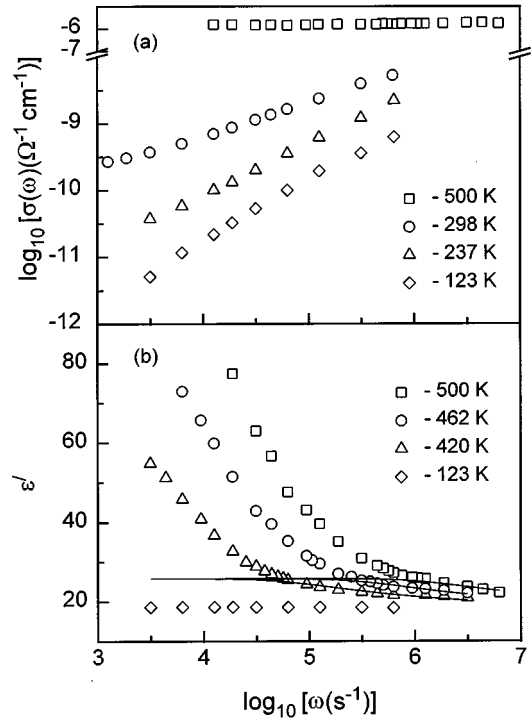


FIG. 3. Variation of measured ac conductivity and dielectric constant with frequency at different temperatures, respectively, for the 30 CuO-70 PbO glass composition. Solid curves in (b) are the best fits to the random-free-energy-barrier model.

$A$  is a temperature-dependent constant and the exponent  $s \leq 1$ . Figure 3(a) also indicates that the exponent  $s$  decreases with the increase of temperature. As pointed out in Sec. I, several models<sup>1-3,12,13</sup> based on quantum mechanical tunneling and classical hopping of charge carriers have been proposed to account for such a frequency-dependent conductivity and its exponent. The model<sup>1,3</sup> based on quantum mechanical tunneling of electrons through a barrier predicts temperature-independent values for  $s$  and thus is not applicable to the present glass system. On the other hand, the model based on classical hopping of electrons<sup>3</sup> over a barrier predicts a decrease of  $s$  with the increase of temperature consistent with our data. The random-free-energy-barrier model<sup>13</sup> is not consistent with the temperature dependence of  $s$ , because this model predicts  $s$  between 0.7 and 1, while our data have values of  $s$  smaller than 0.7; for example  $s = 0.92$  at 80 K and  $s = 0.55$  at 300 K for 30 CuO-70 PbO glass composition. Thus at lower temperatures, classical hopping of electron is the dominant conduction mechanism in the present glass system similar to many transition metal ion glass systems based on conventional network formers<sup>5,6</sup> and thus is not discussed further in detail. At higher temperatures, where the ac conductivity approaches the dc conductivity, it makes no sense to determine the exponent,  $s$ . The data are then discussed in terms of the dielectric relaxation, conductivity relaxation, and random free-energy-barrier models.<sup>13-16</sup>

#### A. Dipolar relaxation model

The frequency dependence of the dielectric constant  $\epsilon'(\omega)$  and loss  $\epsilon''(\omega)$  for the 50 CuO-50 PbO glass composition is

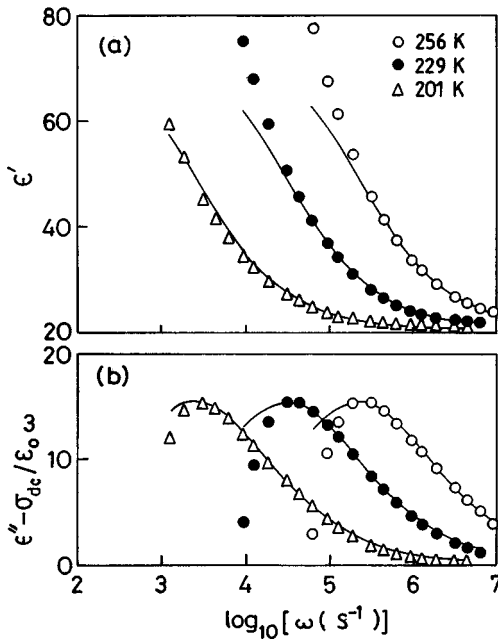


FIG. 4. The frequency dependence of  $\epsilon'$  and  $\epsilon'' - \sigma_{dc}/\epsilon_0\omega$ , respectively, at three different temperatures for the 50 CuO-50 PbO glass composition. Solid curves are the best fits to the dipolar relaxation model.

shown in Figs. 4(a) and 4(b), respectively. The dc contribution  $\sigma_{dc}/\epsilon_0\omega$  (where  $\epsilon_0$  is the free space permittivity) is subtracted from the measured  $\epsilon''(\omega)$  in Fig. 4(b), where a broad loss peak is observed. The dielectric constant and loss data of all glass compositions were fitted to the Cole-Cole function,<sup>14</sup>  $\epsilon^*(\omega) = \epsilon_\infty + (\epsilon_0 - \epsilon_\infty) / [1 + j(\omega\tau_d)^{1-\alpha}]$ , where  $\epsilon_0$  and  $\epsilon_\infty$  are the low- and high-frequency dielectric constants, respectively,  $\tau_d$  is the dielectric relaxation time and  $\alpha$  is the Cole-Cole distribution parameter having values between 0 and 1. The parameters  $\epsilon_0$ ,  $\epsilon_\infty$ ,  $\tau_d$ ,  $\alpha$ , and  $\sigma_d$  were varied to get best fits at different temperatures and frequencies. Such best fits are shown in Figs. 4(a) and 4(b) for 50 CuO-50 PbO

glass composition. The agreement between theoretical and experimental values is very good in the high-frequency tail regime at all temperatures measured. However, the fit in the low-frequency tail is not so good because of the uncertainty involved in the subtraction of the dc contribution from the measured  $\epsilon''(\omega)$ . Similar fits have been observed for other glass compositions. Attempts were also made to fit the dielectric data to the Davidson-Cole function.<sup>15</sup> However, the measured data at all temperatures and frequencies could not be fitted to the Davidson-Cole function. Thus the estimated parameters obtained from the fits of the Cole-Cole function at different temperatures are shown in Table I for the different glass compositions. Table I indicates that the estimated values of  $\alpha$ ,  $\epsilon_0$ , and  $\epsilon_\infty$  for all compositions are almost independent of temperature. It may be noted that the estimated values of  $\epsilon_\infty$  are very close to the experimental values of  $\epsilon'$  calculated at high frequencies and low temperatures. The dc conductivity  $\sigma_d$  estimated from this model is also in agreement with the experimental value of the dc conductivity  $\sigma_{dc}$  (within 2–10 %). It may also be noted in Table I that the values of  $\alpha$  do not show any systematic variation with the glass composition. Comparison with the data for  $\alpha$ ,  $\epsilon_0$ , and  $\epsilon_\infty$  for the transition metal ion glasses formed with conventional network formers,<sup>5</sup> such as  $P_2O_5$ , shows that the values of  $\alpha$  for the present glass compositions are lower than those of  $\alpha$  ( $\geq 0.5$ ) for the conventional glasses and the values of  $\epsilon_0$  and  $\epsilon_\infty$  are much higher than those of the conventional glasses.<sup>4,5</sup> These results clearly show the higher influence of the unconventional network former PbO on the dielectric properties than the conventional formers.<sup>4,5</sup> A lower value of  $\alpha$  is also observed for the 30 CuO–70 PbO glass composition compared with the other glass compositions. An electron microscopic study of these glasses<sup>11</sup> shows that the 30 CuO–70 PbO glass composition is microscopically more homogeneous and thus a decrease of the width of the distributions of relaxation times is observed for this composition.

## B. Conductivity relaxation

The conductivity relaxation model, in which a dielectric modulus is defined by  $M^*(\omega) = 1/\epsilon^*(\omega)$ , can be used to get

TABLE I. Relaxation parameters obtained from dipolar dielectric relaxation model (Cole-Cole equation) (Ref. 14) for different glass compositions at three representative temperatures and the experimental values of  $\sigma_{dc}$  and  $\epsilon_\infty$  (at 100 KHz and 90 K).

Glass composition (mol %)	Temperature (K)	$\tau_d$ (s)	$\alpha$	$\epsilon_\infty$	$\epsilon_0$	$\sigma_d$ ( $10^{-8}$ ) ( $\Omega^{-1} \text{ cm}^{-1}$ )	$\sigma_{dc}$ ( $10^{-8}$ ) ( $\Omega^{-1} \text{ cm}^{-1}$ )	$\epsilon_\infty$ (exp.)
21 CuO-79 PbO	475	$6.30 \times 10^{-5}$	0.40	22	32	2.10	2.12	19.2
	495	$2.80 \times 10^{-5}$	0.40	22	31	5.50	4.47	
	515	$1.40 \times 10^{-5}$	0.40	22	31	9.95	9.85	
30 CuO-70 PbO	420	$2.90 \times 10^{-5}$	0.25	21	34	7.50	4.47	18.5
	462	$6.10 \times 10^{-6}$	0.26	22	33	38.0	27.5	
	500	$1.75 \times 10^{-6}$	0.25	23	32	145	105	
36 CuO-64 PbO	346	$6.25 \times 10^{-4}$	0.46	29	190	1.08	1.00	27.8
	398	$3.50 \times 10^{-5}$	0.44	29	190	16.8	15.0	
	447	$5.00 \times 10^{-6}$	0.44	30	190	120	115	
50 CuO-50 PbO	201	$3.65 \times 10^{-4}$	0.37	21	78	0.26	0.18	21.8
	229	$3.25 \times 10^{-5}$	0.37	21	78	3.65	1.80	
	256	$4.30 \times 10^{-6}$	0.37	21	78	26.0	10.2	

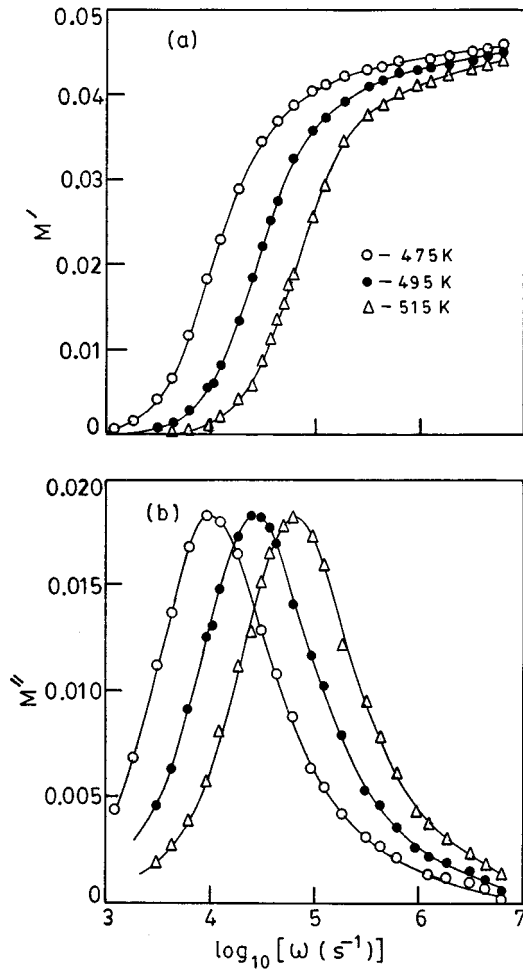


FIG. 5. The frequency variation of  $M'$  and  $M''$ , respectively, at three different temperatures for the 21 CuO-79 PbO glass composition. Solid curves are the best fits to the conductivity relaxation model.

information about the relaxation mechanism in absence of a well-defined dielectric loss peak.<sup>16</sup> Figures 5(a) and 5(b) show the frequency spectra of  $M'(\omega)$  and  $M''(\omega)$  at three different temperatures for 21 CuO-79 PbO glass composition. As the frequency increases,  $M'(\omega)$  increases to a maximum asymptotic value defined as  $M_\infty$ . The spectra of  $M''(\omega)$  show an asymmetric peak approximately centered in the dispersion region of  $M'(\omega)$ . The peak shifts to higher frequencies with the increase of temperature. The frequency  $\omega_c$ , at which the maximum of  $M''(M''_{\max})$  occurs, defines the conductivity relaxation time  $\tau_c$  by  $\omega_c \tau_c = 1$ . The temperature and frequency dependence of  $M'(\omega)$  and  $M''(\omega)$  for the other glass compositions are similar, except for the difference of their magnitudes. The data for  $M'(\omega)$  and  $M''(\omega)$  presented in Fig. 5 have been fitted simultaneously to the theoretical values given by this model using the procedure developed by Moynihan *et al.*<sup>16</sup> In the fitting process the Kohlrausch-Williams-Watts (KWW) function,  $\phi(t) = \exp[-(t/\tau_c)^\beta]$ , have been used,<sup>17-19</sup> where  $\beta$  is a stretching exponent tending to unity for the Debye-type relaxation. This KWW function has been used earlier to describe the relaxation behavior of many ionic and electronic glasses<sup>5,6,9,16,20,21</sup> and polymers.<sup>18,19</sup> A best fit is shown in Fig. 5 for 21 CuO-79 PbO glass. The other glass compositions also showed similar fits. The values of  $\epsilon_\infty$ ,  $\tau_c$ , and  $\beta$  obtained from different glass compositions are shown in Table II. The low-frequency dielectric constant ( $\epsilon_0$ ) and the dc conductivity ( $\sigma_c$ ) were also estimated from the modulus analysis<sup>16</sup> and are shown in Table II. It is seen in Table II that the values of  $\epsilon_0$  and  $\sigma_c$  are close to their experimental values. The composition dependence of the stretching exponent  $\beta$  is shown in Fig. 6 which shows that a very different stretching exponent are obtained for different compositions. Particularly, the  $\beta$  value for the 36 CuO-64 PbO glass is extremely small due to broad asymmetric peak observed in the  $M''(\omega)$  vs  $\log_{10}\omega$  plot (Fig. 7). The broad asymmetric peak observed may be due to the clus-

TABLE II. Relaxation parameters obtained from conductivity relaxation model (Ref. 16) for different glass compositions at three representative temperatures.

Glass composition (CuO mol %)	Temperature (K)	$\tau_c$ (s)	$\beta$	$\epsilon_\infty (= 1/M_\infty)$	$\epsilon_0$	$\sigma_c$ ( $10^{-8} \Omega^{-1} \text{cm}^{-1}$ )
21	475	$8.91 \times 10^{-5}$	0.80	22.2	29.0	1.95
	495	$3.70 \times 10^{-5}$				4.89
	515	$1.58 \times 10^{-5}$				11.0
30	420	$1.84 \times 10^{-5}$	0.77	21.0	28.8	8.68
	462	$3.89 \times 10^{-6}$				41.0
	500	$1.10 \times 10^{-6}$				145
36	346	$2.75 \times 10^{-5}$	0.38	28.7	182	2.40
	398	$1.58 \times 10^{-6}$				41.8
	447	$2.63 \times 10^{-7}$				250
50	201	$6.30 \times 10^{-5}$	0.44	21.4	78.0	1.15
	229	$4.87 \times 10^{-6}$				14.9
	256	$6.16 \times 10^{-7}$				118

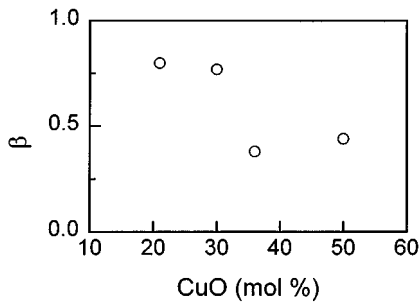


FIG. 6. Variation of stretched exponential parameter,  $\beta$  with the glass composition.

tering of copper ions as observed in electron microscopic studies for this glass composition.

### C. Random-free-energy-barrier model

A random-free-energy-barrier model in which the ac and dc conductivities arise from the same hopping mechanism has been proposed by Dyre,<sup>13</sup> based on the continuous time random walk approximation.<sup>22</sup> The data of the present glass compositions have been analyzed in the light of the random-free-energy-barrier model. The experimental data for  $\epsilon'(\omega)$  and  $\epsilon''(\omega)$  at different temperatures have been fitted by best fit methods simultaneously to

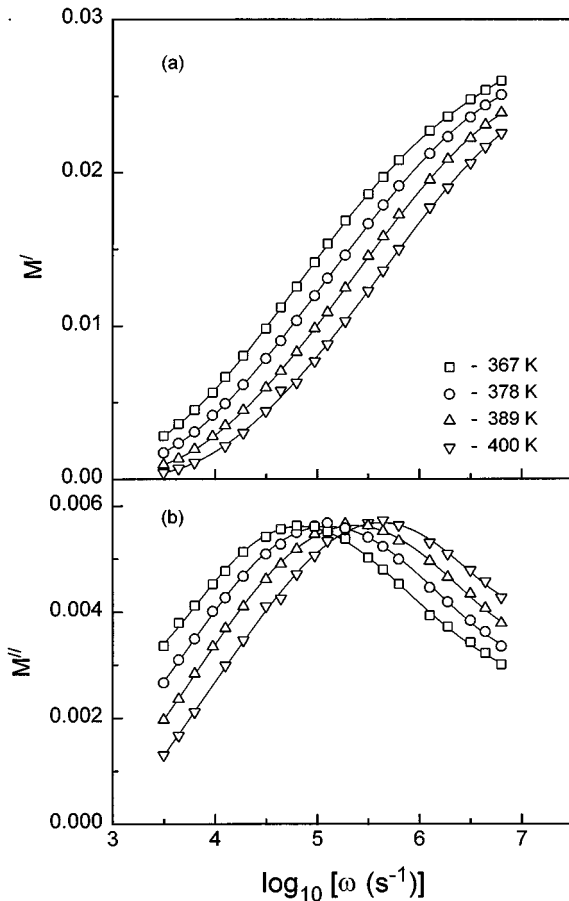


FIG. 7. The frequency variation of  $M'$  and  $M''$ , respectively, at four different temperatures for the 36 CuO-64 PbO glass composition. Solid curves are the best fits to the conductivity relaxation model for  $\beta=0.38$ .

$$\epsilon^*(\omega) = \frac{\sigma_R}{\epsilon_0} \left[ \frac{\tau_R}{\ln(1+j\omega\tau_R)} + \frac{j}{\omega} \right]$$

predicted by this model, using  $\sigma_R$ ,  $\epsilon_\infty$ , and  $\tau_R$  as variable parameters, where  $\sigma_R$  is the dc conductivity predicted by this model and  $\tau_R$  is the relaxation time which is related to the dc conductivity by,  $\epsilon_0\Delta\epsilon = \sigma_R\tau_R/2$ , where  $\Delta\epsilon = \epsilon_0 - \epsilon_\infty$ . A best fit to the dielectric constant  $\epsilon'$  is shown in Fig. 3(b) for a glass composition at three temperatures. It is observed that the fit for this case is worst for low frequencies and high temperatures. However, a reasonable fit (not shown here) to  $\epsilon''$  was observed at all temperatures and frequencies. A worst fit for the 50 CuO-50 PbO glass composition was also observed for both  $\epsilon'(\omega)$  and  $\epsilon''(\omega)$  and the parameters obtained were unreliable. The values for the estimated parameters  $\sigma_R$ ,  $\epsilon_\infty$ , and  $\tau_R$  for all glass compositions except 50 CuO-50 PbO glass, are shown in Table III. The estimated values of  $\epsilon_\infty$  and  $\epsilon_0$  are independent of temperatures. However, the values of  $\epsilon_\infty$  are lower than the experimental values for the glass compositions with higher CuO content and the values of  $\epsilon_0$  are lower than the values obtained from dielectric and conductivity relaxation models. The estimated values of  $\sigma_R$  are in agreement with the experimental values of  $\sigma_{dc}$  within 10–50 % depending on composition and temperatures. Thus the random-free-energy-barrier model cannot predict the dielectric data for the present glass compositions. It is worth noting in Fig. 3 that the dielectric data at low frequencies and high temperatures are influenced by the blocking electrodes and these effects might be the reason for the failure of the random-free-energy-barrier model. The strong increase of the low-frequency data at high temperatures is also not predicted by the conductivity relaxation model. But in this case the low-frequency data are suppressed in the modulus representation.

### D. Temperature dependence of the dc conductivity and relaxation times

The temperature dependence of the dc conductivity in the temperature range of relaxation is shown in Fig. 8 for a glass composition and can be fitted to the Arrhenius equation:  $\sigma_{dc} = \sigma_0 \exp(-W/kT)$ , where  $W$  is the activation energy for the dc conductivity. The dc conductivity for the other glass compositions also showed similar temperature dependence. The activation energy calculated using the equation is shown in Table IV for all glass compositions. It may be noted from Fig. 1 that below the temperature range of dielectric relaxation, the dc conductivity is not Arrhenius. The activation energy decreases with the decrease of temperature which can be accounted for by the polaron hopping theories<sup>23</sup> similar to many other transition metal ion glasses based on conventional network formers.<sup>4,6</sup>

Each of the three models, used to analyze relaxation data, provides characteristic relaxation times (Tables I–III) which have different values. The temperature dependence of the relaxation times obtained from different models is also shown for one glass composition in Fig. 8, where  $\log_{10}(1/\tau)$  is plotted against reciprocal temperature. It is clear that the relaxation times predicted by each model show an activated behavior, i.e., obey the Arrhenius relation  $\tau = \tau_0 \exp(W_r/kT)$ , where  $W_r$  is the activation energy of the

TABLE III. Relaxation parameters obtained from random-free-energy-barrier model (Ref. 13) for different glass compositions at three representative temperatures.

Glass composition (CuO mol %)	Temperature (K)	$\tau_R$ (s)	$\epsilon_0$	$\epsilon_\infty$	$\sigma_R$ ( $10^{-8}$ ) ( $\Omega^{-1} \text{ cm}^{-1}$ )
21	475	$1.05 \times 10^{-4}$	27.7	18.2	2.03
	495	$4.00 \times 10^{-5}$	28.0	18.5	5.61
	515	$1.95 \times 10^{-5}$	28.0	18.0	13.6
30	420	$2.15 \times 10^{-5}$	25.8	16.3	7.83
	462	$4.20 \times 10^{-6}$	25.8	16.3	40.1
	500	$1.10 \times 10^{-6}$	25.8	16.3	153
36	346	$1.26 \times 10^{-3}$	90.0	10.0	1.51
	398	$7.95 \times 10^{-5}$	91.0	10.0	17.7
	447	$1.20 \times 10^{-5}$	93.0	10.0	125

relaxation time and  $\tau_0$  is the high-temperature limit of the relaxation time. The activation energy and  $\tau_0$  for each model are shown in Table IV for all glass compositions. It may be noted that the activation energy is nearly the same in the three cases and is very close to the activation energy for the dc conductivity. The values of the preexponential factor  $\tau_0$ , as expected, are different for the three models, but are of the order of inverse optical phonon frequency determined from the IR spectra.<sup>11</sup> However, how the relaxation times for different models are related or which one is the correct and intrinsic time of the system is unknown at present.

### E. Conduction mechanism

From Tables I–III it is clear that the low-frequency dielectric constant  $\epsilon_0$  predicted by the random-free-energy-barrier model is lower than that predicted by the dipolar and conductivity relaxation models. This model has been already discarded from the quality of fits of the dielectric constant

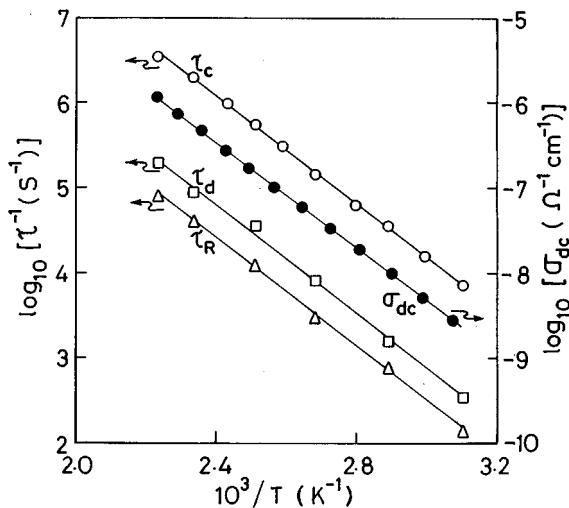


FIG. 8. Temperature dependence of the dc conductivity ( $\sigma_{dc}$ ) and the relaxation times predicted by the dipolar relaxation ( $\tau_d$ ), conductivity relaxation ( $\tau_c$ ), and random-free-energy-barrier ( $\tau_R$ ) models for the 36 CuO-64 PbO glass composition. Solid lines are the least-square straight line fits to the data.

predicted by this model to the experimental data (cf. Sec. III A). The estimated values of  $\epsilon_0$  from the dipolar and conductivity relaxation models are close to one another. It may be noted that the dielectric strength  $\Delta\epsilon = \epsilon_0 - \epsilon_\infty$ , predicted by these models, is much higher for the glass compositions with 36 and 50 mol % CuO than that for the glass compositions with lower CuO content. The physical assumptions implicit in the dipolar and conductivity relaxation models need to be examined to choose the best of these two models. The modulus representation is an averaging procedure for an ensemble of submicroscopic regions with different conductivities and dielectric constants.<sup>16</sup> The closest physical models would be regions in which either the depth of the localized potential wells or site separations differ. The difference in potential barriers would give rise to polarization and a frequency dependent dielectric constant and conductivity. The conductivity relaxation time  $\tau_c = \epsilon_0 \epsilon' / \sigma$  would become a function of  $\sigma$  and  $\epsilon'$  of different regions and thus a distribution of relaxation times is required. The dielectric representation can be based on a similar model involving a random potential well or on conducting path models<sup>24</sup> in which the overall dielectric dispersion arises from the nature of the path taken by the carrier in the materials and the dielectric relaxation arises from the hopping of the charge carriers between localized states. These models also reflect the similarity between the activation energy for dielectric relaxation and dc conductivity.

In transition metal ion glasses the localized states are distributed at random within the tail of an energy band associated with the transition metal ions, where the density of states may be higher than that in more conventional semiconductors. In these glasses the localization is enhanced by polaron formation.<sup>1</sup> At low temperatures, hopping occurs between localized states near the Fermi level (within  $kT$ ). But at higher temperatures in the dispersion regions, hopping occurs between localized states within an appropriate range of energies and site separations lying below and closer to the mobility edges. The conducting path models<sup>24</sup> present a better representation of the physical situation in this case and in this sense dielectric approach is more satisfactory for the present glass compositions. Some authors<sup>25,26</sup> believe that the modulus formalism is wrong, since this formalism forces

TABLE IV. Activation energies ( $W$  and  $W_r$ ) for the dc conductivity ( $\sigma_{dc}$ ) and relaxation times ( $\tau$ ), and preexponential factor  $\tau_0$  predicted by different models for different glass compositions.

Glass composition (CuO mol %)	Temperature range (K)	$\tau_d$		$\tau_c$		$\tau_R$		$\sigma_{dc}$ W (eV)
		$W_d$ (eV)	$\tau_0$ ( $10^{-13}$ ) (s)	$W_c$ (eV)	$\tau_0$ ( $10^{-13}$ ) (s)	$W_R$ (eV)	$\tau_0$ ( $10^{-13}$ ) (s)	
21	465–515	0.80	1.77	0.93	0.18	0.90	0.29	0.82
30	375–500	0.63	8.05	0.63	4.48	0.66	2.19	0.68
36	320–450	0.63	3.42	0.62	0.22	0.63	8.71	0.61
50	185–300	0.35	4.56	0.36	0.54			0.37

an irreversible mixing of separate component  $\sigma$  and  $\epsilon$  as well as needless superposition of information at both low and high frequencies. It is far better to analyze the data in the form of the directly measured quantity conductivity or dielectric constant, where no artefactual frequency-dependent behavior is introduced, as can be the case in the modulus formalism.<sup>26</sup> At the same time it is also unclear if the ac and dc conductivities can be separated as has been done here.<sup>2</sup>

## V. CONCLUSIONS

The frequency-dependent ac conductivity and dielectric properties of the unconventional lead cuprate glasses of different compositions have been investigated over the frequency range  $10^2$ – $10^6$  Hz and temperature range 80–550 K. The analysis of the experimental data shows that at low temperatures, where the ac conductivity is substantially higher than the dc conductivity, the hopping of electrons between localized states near the Fermi level is the dominant loss mechanism. At higher temperatures, the ac conductivity approaches the dc conductivity and the dipolar relaxation

mechanism with a distribution of relaxation times provides a description of the dielectric data quantitatively. The dielectric relaxation occurs due to the hopping of electrons between the localized states within a range of energies near and below the mobility edge. The conductivity relaxation model also provides a good qualitative description of the dielectric data. On the other hand, the random-free-energy-barrier model is not applicable to the present glasses. A higher value of the low- and high-frequency dielectric constants and a narrower distribution of relaxation times have been observed for these unconventional glasses compared with the glasses formed with conventional network former such as  $P_2O_5$  due to the higher influence of the  $Pb^{2+}$  ions of the unconventional network former PbO on the dielectric response than that of the cations of the conventional glass formers.

## ACKNOWLEDGMENT

S.H. acknowledges University Grants Commission (India) for providing him financial support.

\*Author to whom correspondence should be addressed.

<sup>1</sup>N. F. Mott and E. A. Davis, *Electronic Processes in Non-Crystalline Materials*, 2nd ed. (Clarendon, Oxford, 1979), p. 225.

<sup>2</sup>A. R. Long, *Adv. Phys.* **31**, 553 (1982).

<sup>3</sup>S. R. Elliott, *Adv. Phys.* **36**, 135 (1987).

<sup>4</sup>M. Sayer and A. Mansingh, *Phys. Rev. B* **6**, 4629 (1972); *Phys. Chem. Glasses* **23**, 83 (1982).

<sup>5</sup>A. Mansingh, R. P. Tandon, and J. K. Vaid, *Phys. Rev. B* **21**, 4829 (1980); *J. Phys. C* **9**, 1809 (1976); A. Mansingh, *Bull. Mater. Sci.* **2**, 325 (1980).

<sup>6</sup>A. Ghosh, *Phys. Rev. B* **41**, 1479 (1990); **42**, 5665 (1990); **45**, 11 318 (1992).

<sup>7</sup>G. S. Linsley, A. E. Owen, and F. M. Hayatee, *J. Non-Cryst. Solids* **4**, 228 (1970); A. I. Lakatos and M. Abkowitz, *Phys. Rev. B* **3**, 1791 (1971); A. E. Owen and J. M. Robertson, *J. Non-Cryst. Solids* **4**, 208 (1970).

<sup>8</sup>I. Thurzo, B. Baranock, and J. Donpovec, *J. Non-Cryst. Solids* **28**, 177 (1978).

<sup>9</sup>A. Mansingh, V. K. Dhawan, and M. Sayer, *Philos. Mag. B* **48**, 215 (1983).

<sup>10</sup>S. Hazra and A. Ghosh, *Phys. Rev. B* **51**, 851 (1995).

<sup>11</sup>A. Ghosh, *Bull. Mater. Sci.* **18**, 53 (1995).

<sup>12</sup>M. Pollak, *Philos. Mag.* **23**, 519 (1971); A. L. Efros, *ibid.* **23**, 519

(1971); G. E. Pake, *Phys. Rev. B* **6**, 1571 (1972).

<sup>13</sup>J. C. Dyre, *Phys. Lett. A* **108**, 457 (1987); *J. Appl. Phys.* **64**, 2456 (1988).

<sup>14</sup>K. S. Cole and R. H. Cole, *J. Chem. Phys.* **9**, 341 (1941).

<sup>15</sup>D. V. Davidson and R. H. Cole, *J. Chem. Phys.* **19**, 1484 (1951).

<sup>16</sup>P. B. Macedo, C. T. Moynihan, and R. Bose, *Phys. Chem. Glasses* **13**, 171 (1972); C. T. Moynihan, L. P. Boesch, and N. L. Laberage, *Phys. Chem. Glasses* **14**, 122 (1973).

<sup>17</sup>R. Kohlrausch, *Pogg. Ann.* **12**, 393 (1847).

<sup>18</sup>G. Williams and D. C. Watts, *Trans. Faraday Soc.* **66**, 80 (1970).

<sup>19</sup>G. Williams, D. C. Watts, S. B. Dev, and A. M. North, *Trans. Faraday Soc.* **67**, 1323 (1971); G. Williams and P. J. Hains, *Faraday Symp. Chem. Soc.* **6**, 14 (1972).

<sup>20</sup>S. W. Martin, *Appl. Phys. A* **49**, 239 (1989).

<sup>21</sup>K. L. Ngai and S. W. Martin, *Phys. Rev. B* **40**, 15 (1989); **40**, 10 550 (1989); K. L. Ngai, *Solid State Ionics* **5**, 27 (1981); S. Martin and C. A. Angel, *J. Non-Cryst. Solids* **83**, 185 (1986).

<sup>22</sup>E. W. Montroll and G. H. Weiss, *J. Math. Phys.* **6**, 167 (1965).

<sup>23</sup>D. Emin, *Phys. Rev. Lett.* **33**, 303 (1974); J. Schnakenberg, *Phys. Status Solidi* **28**, 623 (1968).

<sup>24</sup>H. Namikawa, *J. Non-Cryst. Solids* **18**, 173 (1975); K. Shimakawa, *ibid.* **43**, 145 (1981).

<sup>25</sup>J. C. Dyre, *J. Non-Cryst. Solids* **135**, 219 (1991).

<sup>26</sup>S. R. Elliott, *J. Non-Cryst. Solids* **170**, 97 (1994).